J Mater Sci: Mater Med
DOI 10.1007/s10856-013-4942-1

Preparation of methotrexate-loaded, large, highly-porous PLLA microspheres by a high-voltage electrostatic antisolvent process

Ai-Zheng Chen · Yue-Mei Yang · Shi-Bin Wang · Guang-Ya Wang · Yuan-Gang Liu · Qing-Qing Sun

Received: 31 July 2012 / Accepted: 29 April 2013

Abstract A high-voltage (10 kV) electrostatic antisolvent process was used to prepare methotrexate (MTX)-loaded, large, highly-porous poly-L-lactide (PLLA) microspheres. MTX solution in dimethyl sulfoxide (DMSO) and PLLA solution in dichloromethane (DCM) were homogeneously mixed, and then ammonium bicarbonate (AB) aqueous solution was added. The mixed solution was emulsified by ultrasonication with Pluronic F127 (PF127) as an emulsion stabilizer. The emulsion was electrosprayed by the specific high-voltage apparatus and dropped into a 100 mL of ethanol, which acted as an antisolvent for the solute and extracted DMSO and DCM, causing the co-precipitation of PLLA and MTX, thus forming microspheres with AB aqueous micro-droplets uniformly inlaid. The obtained MTX–PLLA microspheres were subsequently lyophilized to obtain large, highly-porous MTX–PLLA microspheres, which exhibited an identifiable spherical shape and a rough surface furnished with open pores, with a mean particle size of 25.0 μm, mass median aerodynamic diameter of 3.1 ± 0.2 μm, fine-particle fraction of 57.1 ± 1.6 %, and porosity of 81.8 %; furthermore, they offered a sustained release of MTX. X-ray diffraction and Fourier transform-infrared spectra revealed that no crystallinity or alteration of chemical structure occurred during the high-voltage electrostatic antisolvent process, which in this study was proved to have great potential for preparing highly-porous drug-loaded polymer microspheres for use in pulmonary drug delivery.

A.-Z. Chen (✉) · Y.-M. Yang · S.-B. Wang (✉) · G.-Y. Wang · Y.-G. Liu · Q.-Q. Sun
College of Chemical Engineering, Huaqiao University, Xiamen 361021, China
e-mail: azchen@hqu.edu.cn

S.-B. Wang
e-mail: sbwang@hqu.edu.cn

A.-Z. Chen · S.-B. Wang · Y.-G. Liu
Institute of Biomaterials and Tissue Engineering, Huaqiao University, Xiamen 361021, China

1 Introduction

Large, highly-porous microspheres (LHPMs) have been intensively investigated as promising pulmonary drug-delivery devices in recent years [1–5]. This ever-growing interest can be ascribed to three reasons. First, the mean MMAD of LHPMs lies in the range of 1–5 μm [6], which can mitigate particle aggregation before inhalation and decrease the possibility of the particles being exhaled, thereby increasing the pulmonary deposition efficiency and overcoming mucociliary clearance [7]. Second, due to the size-discriminating particle uptake properties of alveolar macrophages [8], the large geometric diameter (5–30 μm) of LHPMs can efficiently prevent them being taken up and cleared by alveolar macrophages [9]. Third, drug-loaded LHPMs can offer controlled release of drug agents over a prolonged period, either for local lung therapy or systemic therapy, greatly reducing the administration frequency [10].

Conventional strategies to fabricate LHPMs are represented by a spray-drying method [11] and a double emulsion method [9]. For both processes, the selection of appropriate pore-forming agents, such as water-soluble osmogens [9], extracted porogens [12], and effervescent agents [13], is a tough challenge and actually plays a crucial role in determining the detailed porous structure of the obtained microspheres. Furthermore, spray drying is not suitable for treatment with temperature-sensitive

Published online: 10 May 2013

compounds, and the properties of the prepared particles are not easily controllable. As for the double emulsion method, the corresponding procedures are always very tedious, comprising a troublesome subsequent separation procedure of microspheres from the aqueous phase; also, the particle size distribution of the products is relatively wide. Apart from that, non-degradable stabilizers, for instance, polyvinyl alcohol (PVA), are commonly added, which requires additional removal.

High-voltage electrostatic-based techniques have shown great potential in particle engineering because of their advantages, including a controllable particle shape, surface morphology, and particle size, as well as the production of particles with good dispersibility [14, 15]. Many researchers have reported on electrospraying encapsulation: Zhang and He [16] successfully encapsulated living cells into alginate microcapsules by electrostatic spraying and carried out in-depth investigation of the operating parameters; Zhou et al. [17] employed electrostatic spraying to prepare hepatocyte-entrapped polyelectrolyte microcapsules, with diameters of 200–800 μm and a narrow size distribution. However, few reports in the literature deal with porous polymer microspheres created by electrospraying.

In this study, we attempted to use a high-voltage electrostatic antisolvent process to prepare drug-loaded, large, highly-porous polymeric microspheres with a low density ($\rho < \sim 0.4$ g/cm^3) and an appropriate MMAD (1–5 μm) for pulmonary drug delivery. MTX, an antifolate drug which is nearly insoluble in water and has comprehensive pharmacological effects against cancer and autoimmune diseases, was selected as a drug model. PLLA and AB were used as the structure matrix and pore-forming agent, respectively. Blank LHPMs and MTX-loaded LHPMs were prepared and their physicochemical characterization was investigated by scanning electron microscopy (SEM), XRD, and FTIR. The corresponding aerodynamic properties, drug loads, encapsulation efficiencies, and drug release profiles were also evaluated.

2 Experimental section

2.1 Materials

PLLA (Mw 50,000, 1.5 dl/g) was purchased from the Jinan Daigang Co., Ltd (Jinan, China). PF127 and AB were purchased from Sigma-Aldrich (USA). MTX was provided by the Surui Pharmaceutical Co., Ltd (Suzhou, China). DCM and DMSO were all obtained from the Sinopharm Chemical Reagent Co., Ltd. All other compounds were of analytical purity.

2.2 Methods

2.2.1 *High-voltage electrostatic antisolvent process*

Figure 1 shows a schematic diagram of the high-voltage electrostatic droplet generator apparatus, which consists of a high-voltage power supply (made in the University of Shanghai for Science and Technology), a 10 mL plastic syringe with a blunt stainless steel nozzle (26 G, inner diameter = 0.24 mm), a microinfusion pump (AJ5805, the Shanghai Anji Electronic Equipment Co., Ltd, China), and a flat metal container as a collector, placed at a fixed distance (4 cm) from the nozzle tip. In the running of the experiment, droplets were produced by syringe pump extrusion (50 mm/h) into approximately 100 mL of an antisolvent of absolute ethanol to form the polymer microspheres in the 10 kV voltages. The positive electrode of the high-voltage power supply was attached to the tip of the nozzle and the negative electrode to the collector when a fluid jet was ejected.

2.2.2 *Preparation of blank and MTX-loaded porous PLLA microspheres*

A 0.5 mL sample of freshly-prepared AB solution (300 mg/mL) and 5 mL of PLLA DCM solution (30 mg/mL) containing PF127 (30 mg/mL) as an emulsion stabilizer were mixed and sonicated using an Ultrasonic Processor (JY 92-ΠD, the Ningbo Xingzhi Biological Technology Co., Ltd., China) for 30 s, alternating on and off (total sonication time: 1 min) at 200 W of power and 25 °C, resulting in the formation of a water-in-oil (W/O) emulsion. The sonicated W/O emulsion was immediately transferred to the plastic syringe.

When the voltage, distance between the nozzle and the metal collector, and pre-set flow rate of emulsion were stabilized at 10 kV, 4 cm, and 50 mm/h, respectively, the obtained emulsion began being extruded from the syringe pump, electrostatically sprayed, and injected into 100 mL of ethanol. Then, the PLLA microspheres, embedding AB aqueous micro-droplets, were formed and subsequently stirred for 1 h at 25 °C and lyophilized (100 Pa and −80 °C) for 24 h to generate blank, large, highly-porous PLLA microspheres.

To entrap MTX into the porous PLLA matrix, MTX (100 mg/mL) was dissolved in DMSO and then added to the PLLA solution (30 mg/mL) in DCM; this was followed by sonication for 1 min (alternating 30 s on and off, 200 W power, 25 °C). After that, 0.5 mL of AB solution (300 mg/mL) and PF 127 (final concentration of 30 mg/mL) were added to the resulting mixed solution and sonicated for 1 min (alternating 30 s on and off, 200 W power, 25 °C). The subsequent process, the same as that illustrated above,

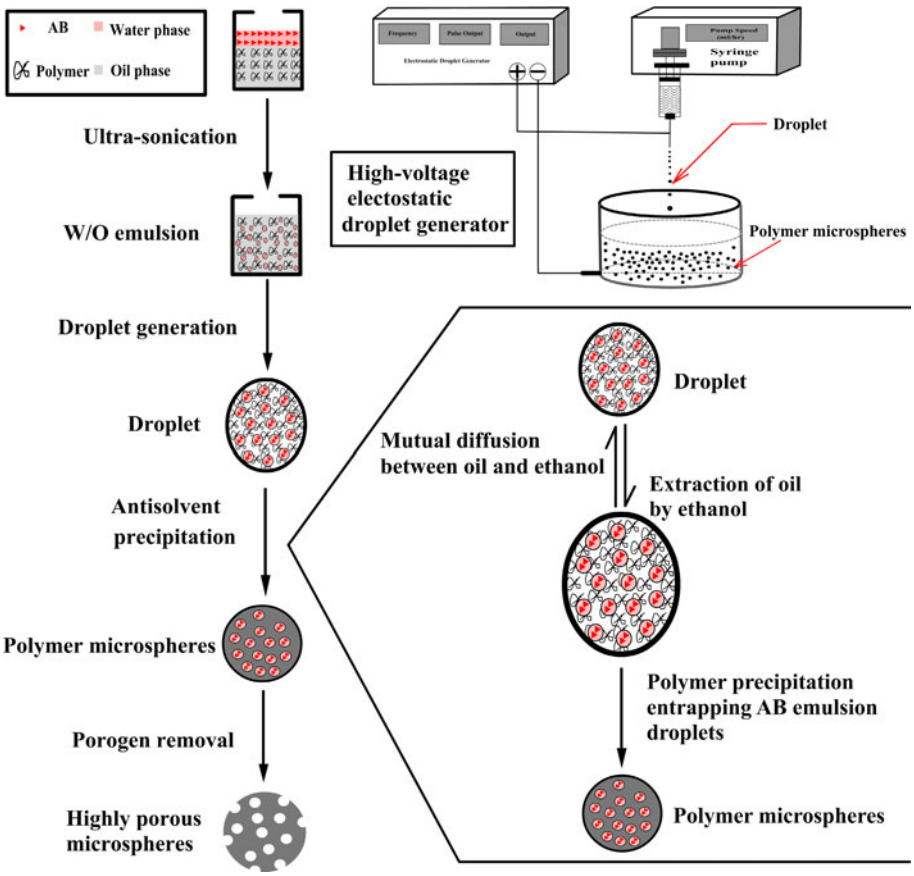

Fig. 1 Schematic description of the apparatus and preparation process of porous microspheres

was performed to generate MTX-loaded, large, highly-porous PLLA microspheres.

2.2.3 *Surface morphology and particle size distribution*

The external and internal surface morphologies of the porous PLLA microspheres and porous MTX–PLLA microspheres were examined by SEM (S-4800 UHR FE-SEM, Hitachi). Dry microspheres were attached to specimen stubs using double-sided tape and sputter-coated with gold–palladium under vacuum. The mean diameter of the microspheres and its standard deviation were obtained by analyzing the SEM images with Image-Pro-Plus 6.0 and Origin 8.5.

2.2.4 *Investigation of aerodynamic properties*

In accordance with the literature [18, 19], the aerodynamic properties of the porous PLLA microspheres and porous MTX–PLLA microspheres were determined using an eight-stage MarkII Anderson Cascade Impactor (ACI, Thermo Scientific, USA). The cumulative mass of powder less than the effective cutoff diameter as percent of total mass recovered in the ACI was plotted against the effective cutoff diameter. MMAD was defined as the particle size at which the line crossed the 50th percentile.

The FPF was defined as the amount of powder with an aerodynamic size <4.7 μm divided by the initial total powder. The porosity and pore size distribution of the PLLA porous microspheres were determined using a high-pressure mercury intrusion porosimeter (Quantachrome Instrument Co.).

2.2.5 *XRD and FTIR measurements*

XRD measurements of the original PLLA and the porous PLLA microspheres were carried out using a Panalytical's X'pert PRO diffractometer. The measurements were performed in the range of 5–50° with a step size of 0.02° s^{-1} in 2θ using Cu kα radiation as the source. FTIR spectra were obtained using an FTIR-8400S analyzer (Shimadzu, Japan). For each sample, 256 scans were collected at a resolution of 2 cm^{-1} over the wavenumber region of 4000–400 cm^{-1}.

2.2.6 *Determination of drug load and encapsulation efficiency*

Approximately 10 mg of porous MTX–PLLA microspheres, accurately weighed, were dissolved in 5 mL of DCM; then 10 mL of phosphate buffered saline solution (PBS, pH 7.4) was added and stirred by a magnetic force

stirrer to volatilize the DCM. The resulting solution was filtrated through a 0.22 μm membrane, and the amount of encapsulated MTX was analyzed using a UV spectrophotometer (the Hong Kong Yongxian Electronic Instrument Co., Ltd.) at 302.8 nm. According to the Pharmacopeia of People's Republic of China (2010), the drug load and encapsulation efficiency were calculated by Eqs. (1) and (2), respectively.

$$\text{Drug load} = \frac{W_1}{W_2} \times 100\% \quad (1)$$

$$\text{Encapsulation efficiency} = \frac{W_3 - W_4}{W_3} \times 100\% \quad (2)$$

where W_1 is the weight of the MTX encapsulated in the microspheres, W_2 is the gross weight of the microspheres, W_3 is the total weight of MTX used in the process, and W_4 is the weight of MTX in the liquid medium. Each experiment was carried out in triplicate.

2.2.7 *Studies of drug release profiles*

Approximately 30 mg of porous MTX–PLLA microspheres were placed in the pretreated dialysis bag (molecular weight cut-off: 8,000–14,000), which was hung in a 50 mL centrifuge tube with 10 mL of PBS (pH 7.4) and incubated in a shaking water bath at 37 °C at 60 rpm. Three milliliters of solution was periodically removed and the amount of MTX was analyzed using a UV spectrophotometer at 302.8 nm. The volume of solution was kept constant by adding fresh medium. Release profiles were calculated in terms of the cumulative release percentage of MTX (%, w/w) with incubation time. Each experiment was carried out in triplicate.

3 Results and discussion

3.1 Preparation of blank and MTX-loaded porous PLLA microspheres

Both blank and MTX-loaded highly-porous PLLA microspheres have been successfully prepared by the high-voltage electrostatic antisolvent process. The brief mechanism of the preparation process is shown in Fig. 1.

In the running of the experiment, a 10 kV voltage was placed between the syringe nozzle and the metal collector, forming an electrostatic field with a high field intensity. When the emulsion was extruded by a constant hydrostatic pressure from the syringe nozzle at the preset flow rate, a high voltage began being applied to the liquid and a large electrostatic charge began to be concentrated on the surface of the droplets. Repulsion of the like charges on the surface of the droplets worked to pull the droplet apart; however, this repulsion was also counterbalanced by the intermolecular forces which are determined by the molecular properties, including polarity, symmetry, and molecular weight [20]. At a critical charge strength, coulombic forces prevailed and the large droplets were split into quantities of smaller satellites that would continue falling down due to the repulsion force and gravity. The critical charge strength was satisfied by a large enough surface-charge density of the droplets, which was determined by the droplet size and voltage used. That meant that the smaller satellites would continue being split until they were small enough to allow the repulsion force of like charges and intermolecular forces to be balanced with each other [21].

The electrosprayed droplet was a micro-emulsion system, comprising a PLLA–DCM solution as the external phase and universally inlaid and dispersed AB aqueous micro-droplets as the internal phase. In the initial emulsion and this micro-emulsion system, AB and PF127 may work synergistically as emulsion stabilizers to reduce the water–oil interfacial tension and impede the aggregation of the dispersed AB aqueous micro-droplets. Due to the micro-scale size, the surface-to-volume ratio of the electrosprayed droplets was very large, which could accelerate the evaporation of oil solvent (DCM); however, the repulsion force and gravity of the droplets speeded the droplets' fall, and the short distance between the syringe and the collector also limited their floating time. Thus, the effect of DCM evaporation in this process on solidification of the electrosprayed droplets could be negligible compared with DCM extraction by ethanol in the subsequent process.

When the micro-emulsion droplets were electrosprayed and dripped into the large volume of ethanol (a nonsolvent for PLLA), rapid mutual diffusion between the oil solvent (DCM) and extractant (ethanol) occurred, which increased the saturation of the PLLA–DCM solution, caused fast polymer precipitation entrapping AB emulsion droplets, and finally formed PLLA microspheres. At this moment, rapid precipitation of PLLA could not only lead to volume shrinkage of the PLLA microspheres compared with the electrosprayed micro-emulsion droplets, but also shift the position and alter the distribution of the inlaid AB aqueous micro-droplets, making some closer together and others further apart. This kind of position and distribution alteration of inlaid AB droplets could be a potential reason for the cross-section inside the PLLA matrix.

In the lyophilization process, the low pressure and temperature (100 Pa and −80°, respectively) enhanced the sublimation of water in the inlaid aqueous droplets, which induced and boosted the decomposition of AB into NH_3, CO_2, and H_2O. Sublimation of water and volatilization of NH_3 and CO_2 left empty pores in the PLLA matrix and release of the resulting gas opened pores on the surface of the PLLA microspheres. The cross-section inside the

PLLA matrix could be made by a gas burst or by removal of partially conjuncted AB aqueous micro-droplets.

As for the preparation of MTX-loaded porous PLLA microspheres, extraction of the solvent (DMSO and DCM) by ethanol resulted in co-precipitation of MTX and PLLA. However, due to the different precipitation speeds, it is hardly possible for MTX and PLLA to be precipitated into a homogenous phase. That is, MTX could be absorbed or just loosely bound onto the external and internal surfaces of the PLLA matrix, or completely entrapped into the PLLA matrix, both of which would affect the drug encapsulation efficiency and drug release profile.

3.2 Surface morphology and particle size distribution

Well-dispersed and identifiably spherical-shaped microspheres were prepared by the high-voltage electrostatic antisolvent process. To better emphasize the pore-forming function of AB, non-porous PLLA microspheres were prepared without the addition of AB into the inner water phase in the initial emulsion. As shown in Fig. 2a–c, AB did not affect the spherical shape of the three kinds of microspheres; the surface of the non-porous PLLA microspheres (prepared without the addition of AB, Fig. 2a) looked remarkably smoother, with a few spile-holes which could be caused by water lyophilization. As for the MTX-loaded (5 % drug dosage) and blank porous PLLA microspheres (both prepared with an AB/PLLA ratio of 1:1), no significant difference was observed in their surface morphology: both appeared rough and were furnished with quantities of open pores possessing various diameters; the interior of the microspheres was full of cavities, left by the removal of AB aqueous micro-droplets and release of H_2O, NH_3, and CO_2. These results demonstrate that it is AB that worked as an efficient pore-forming agent in the high-voltage electrostatic anti-solvent process, and the effect of entrapped MTX on the microsphere surface morphology and pore size was negligible.

The particle size of the non-porous and blank porous PLLA microspheres ranged from 5.0 to 35.0 μm, with a narrow particle size distribution and a mean particle size of 20.0 ± 0.9 μm. The 5 % MTX-loaded porous PLLA microspheres exhibited a larger particle size, ranging from 10 to 50 μm, with an average of 25.0 μm. This result can be explained by the fact that AB, although working efficiently to burst out pores, did not have any effect on the particle size of the microspheres; also, the MTX solution in DMSO may alter the surface tension and viscosity of the initial emulsion and, in turn, shift the balance of surface like-charges repulsion and intermolecular forces, and thereby increase both the micro-emulsion droplet volume and the size of the obtained drug-loaded porous microspheres, though not so significantly.

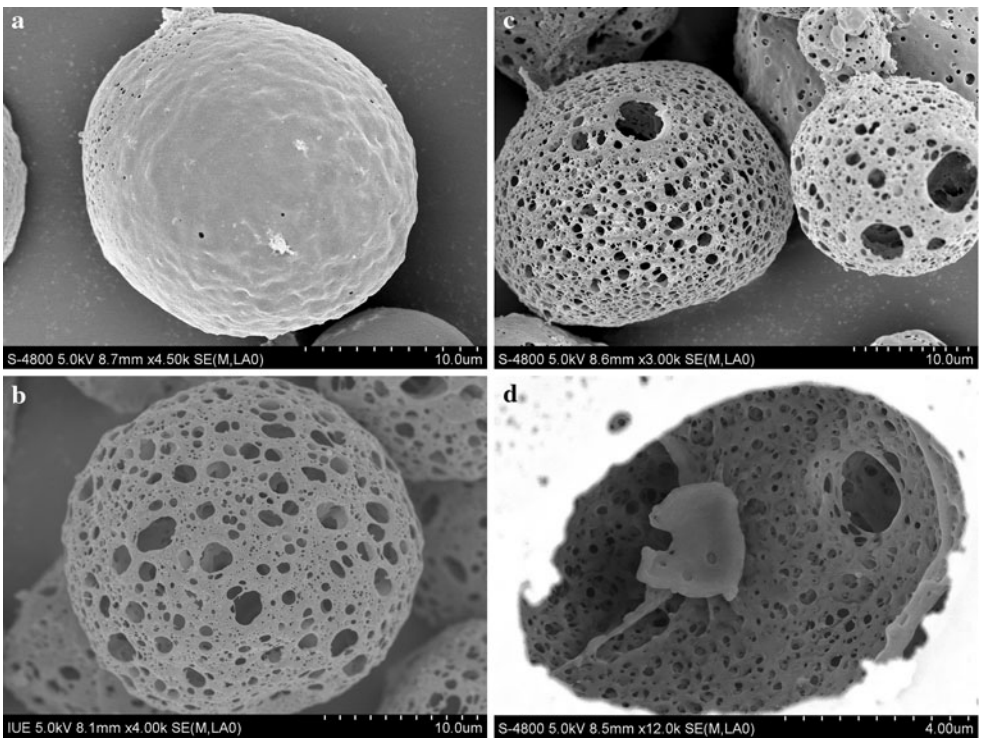

Fig. 2 SEM photomicrograph of **a** non-porous PLLA microspheres; **b** porous PLLA microspheres; **c** porous MTX–PLLA microspheres; **d** internal surface of porous PLLA microspheres

Table 1 Preparation conditions and particle size distributions of porous PLLA microspheres (a) and porous MTX–PLLA microspheres (b)

Samples	PLLA (mg/mL)	AB (mg/mL)	AB/PLLA (w/w)	Dg (μm)	MMAD (μm)	FPF < 4.7 μm (%)
a	30	300	1.0	19.6 ± 0.7	2.9 ± 0.2	54.2 ± 2.2
b	30	300	1.0	26.1 ± 0.5	3.1 ± 0.2	57.1 ± 0.6

Values are represented as mean ± standard deviation of the mean ($n = 3$)

PLLA poly-L-lactide, *AB* ammonium bicarbonate, *Dg* geometrical diameter, *MMAD* mass median aerodynamic diameter, *FPF* fine-particle fraction

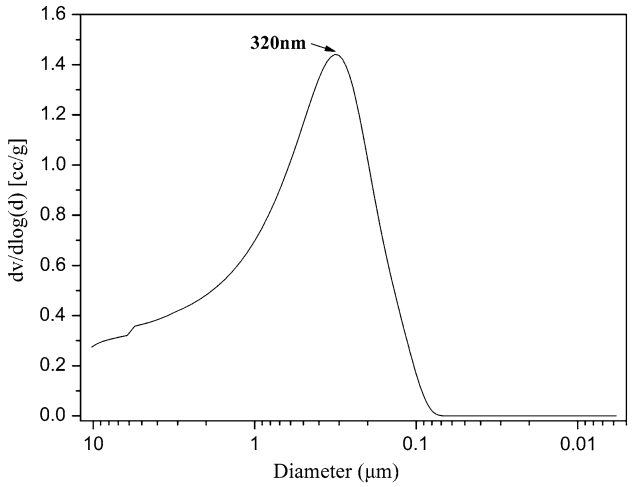

Fig. 3 Internal pore size distribution of porous PLLA microspheres

As shown in Fig. 2, the MTX-loaded porous PLLA microspheres possessed a large volume (mean of 25.0 μm) and quantities of surface pores and crossing internal cavities, which not only significantly reduce its density and improve its aerodynamic properties, but also contribute greatly to the avoidance of macrophage uptake.

3.3 Aerodynamic properties and porosity

The aerodynamic diameter was regarded as a key factor for pulmonary drug delivery, especially for inhaled polymer microspheres [19, 22]. In particular, for large, porous polymer microspheres, improved aerosolization properties helps to obtain high deposition efficiency in the lung epithelium and a large volume can avert alveolar macrophage clearance and increase bioavailability.

As shown in Table 1, the aerodynamic properties showed no significant difference between MTX-loaded and blank porous PLLA microspheres. The MMAD and FPF of blank porous PLLA microspheres were 2.9 ± 0.2 μm and 54.2 ± 2.2 %, respectively, whereas the MMAD of the porous MTX–PLLA microspheres was 3.1 ± 0.2 μm and the FPF was 57.1 ± 1.6 %. The slightly larger MMAD in the porous MTX–PLLA microspheres could be attributed to the density increase [23] caused by the addition of MTX. As the MMAD reached approximately 3 μm and the FPF was more than 50 %, the porous PLLA microspheres were expected to be deposited in the deep lung with greater efficiency. Thus, the high-voltage electrostatic antisolvent process could produce polymer porous microspheres with favorable aerodynamic properties, which would be preponderant, especially in large-scale production.

The porosity of porous PLLA microspheres prepared with an AB/PLLA ratio of 1.0 reached 81.8 %. As shown in Fig. 3, the interior pore size of porous PLLA microspheres ranged from 53.4 nm to 10.2 μm, with a mean pore size of 320 nm. From Fig. 2d, it can be seen that the size of the homogeneous pores in the internal surface of the porous microspheres was approximately 200–400 nm. In the lyophilization process, sublimation of water and volatilization of NH_3 and CO_2 left empty pores in the PLLA matrix, and release of the resulting gas opened pores on the microspheres' surface. Removal of partially conjuncted AB aqueous micro-droplets and internal gas-burst caused interconnected pores inside the PLLA matrix. The large volume and high porosity of the obtained MTX-loaded PLLA microspheres could not only couple high deposition efficiency in the deep lung with alveolar macrophage uptake resistance, but also offer potential for controlled entrapped-drug release [24].

3.4 XRD and FTIR measurements

The XRD and FTIR spectra of the original PLLA and porous PLLA microspheres were collected. The XRD clearly reveals that the polymer crystallinity was unchanged (Fig. 4). The FTIR spectra of PLLA indicate a broad band at 1,700–1,900 cm^{-1}, with the characteristic peak centered at 1759 cm^{-1}, which should be ascribed to carbonyl vibrational stretching and demonstrates the existence of PLLA. After the high-voltage electrostatic antisolvent process, neither broadening of the band nor a shift in the peaks was observed in the FTIR spectra of the porous PLLA microspheres, indicating no significant perturbation of the chemical structure (Fig. 5). The results reveal that almost none of the PF127, the W/O emulsion stabilizer, was present in the porous microspheres' matrix; this is probably because the PF127 was extracted by ethanol in the antisolvent process. These results demonstrate that the

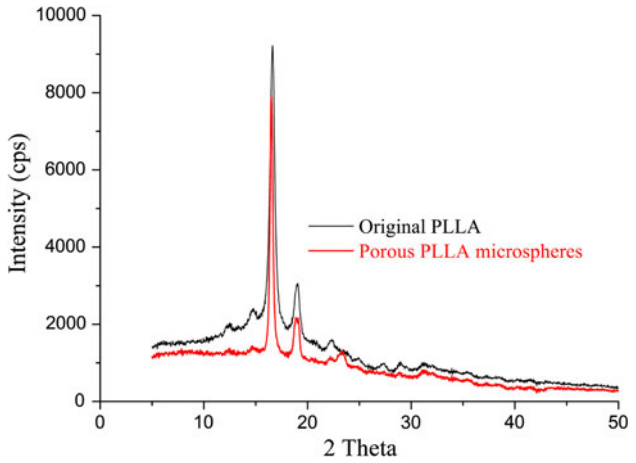

Fig. 4 XRD spectra of original PLLA and porous PLLA microspheres

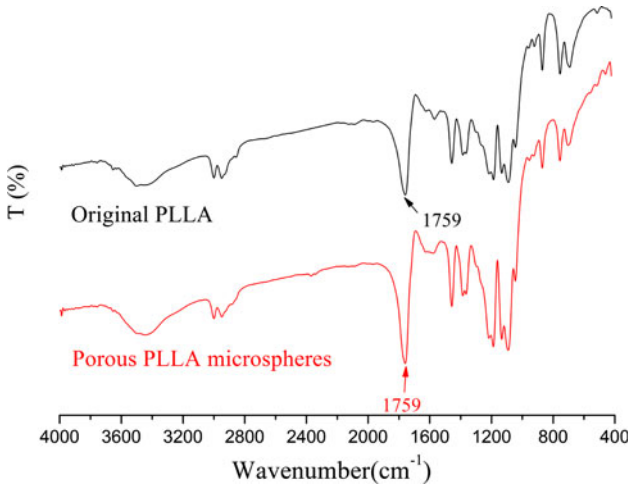

Fig. 5 FTIR spectroscopy of original PLLA and porous PLLA microspheres

high-voltage electrostatic antisolvent process is a typically physical process, which cannot alter the crystallinity or chemical structure of the agents used.

3.5 Drug load and encapsulation efficiency

MTX was encapsulated into porous PLLA microspheres with an AB/PLLA ratio of 1:1. When theoretical drug loads of 2.5, 5 and 10 % MTX were employed, the corresponding encapsulation efficiencies were 39.5, 35.3, and 22.9 %, respectively, as shown in Fig. 6. The drug load of the porous MTX–PLLA microspheres increased with the increase in the MTX dose, whereas the corresponding encapsulation efficiency decreased. The results indicate that the high-voltage electrostatic antisolvent process could be used as a new strategy to entrap MTX into PLLA to form porous MTX–PLLA microspheres.

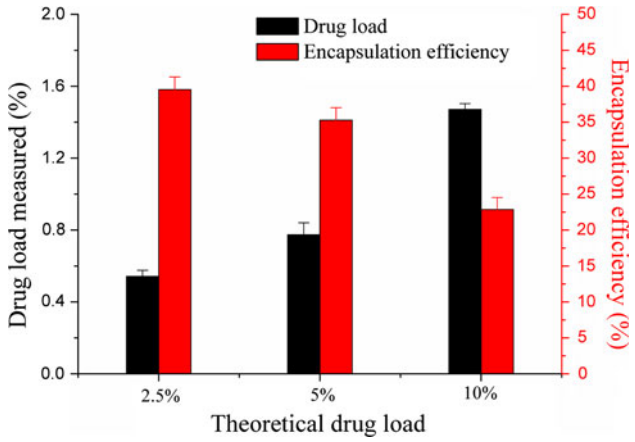

Fig. 6 Drug load and encapsulation efficiency of porous MTX–PLLA microspheres (*bar* indicates S.D., $n = 3$)

The higher drug dosage will result in more MTX being precipitated and thereby increase the corresponding drug load. For the encapsulation efficiency, PLLA would be precipitated faster than MTX; that is, some MTX would be co-precipitated with and entrapped into PLLA, and the MTX that was precipitated later, perhaps a larger amount, would have to be precipitated onto the external or internal surface of the PLLA matrix; under this condition, the higher the drug dosage, the lower the encapsulation efficiency. Furthermore, this type of precipitation and the resulting combination form of PLLA and MTX will also affect the drug release profile.

3.6 Drug release studies

In vitro MTX release was performed in PBS (pH 7.4) incubated at 37 °C, and the amount of MTX was determined using the UV spectrophotometer. Figure 7 shows the in vitro MTX release profile of raw MTX powder and porous MTX–PLLA microspheres prepared with different drug dosages of 2.5, 5 and 10 %.

As shown in Fig. 7, the drug release profiles of porous MTX–PLLA microspheres are significantly distinguished from that of raw MTX powder. MTX release from raw powder was completed within 2 h. Generally, two potential therapy hazards could be caused by this kind of release profile. First, complete release within a short period could lead to a high drug concentration in an instant, which stimulates and enhances the metabolic drug clearance of the body and thereby greatly reduces drug bioavailability [25, 26]. Second, this uncontrolled burst release, especially of anticancer drugs (e.g., MTX), could result in a local drug concentration that is too high, which not only hampers the drug's targeted delivery, but also severely jeopardizes local tissues [27].

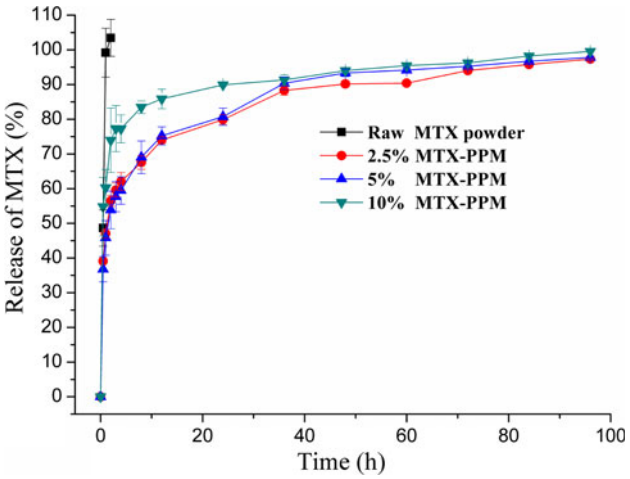

Fig. 7 Cumulative drug release curve of porous MTX–PLLA microspheres (*bar* indicates S.D., $n = 3$)

Taken as a whole, the drug release of MTX-loaded highly-porous PLLA microspheres was biphasic, with an initial burst release followed by a much slower release period. For the 10 % porous MTX–PLLA microspheres, the accumulative drug release was 50 % within the first 30 min, then reached more than 80 % in 36 h, and finally shifted to a flat stage in the next 60 h. Accumulative MTX release curves of the 2.5 and 5 % porous MTX–PLLA microspheres were almost overlapped, with 30 % within the first 30 min, 90 % within 40 h, and complete release after 100 h. In the initial 40 h, 10 % MTX–PLLA microspheres released MTX remarkably faster than 2.5 and 5 % MTX–PLLA microspheres. After that, the MTX was all slowly given out until the release was complete.

The initial burst release of MTX-loaded porous PLLA microspheres can be explained by the fact that different precipitation speeds of MTX and PLLA led to phase separation and left some MTX absorbed onto or loosely bound with the PLLA matrix surface. This surface-adhered MTX gave a burst release the moment the drug-loaded porous microspheres came into contact with the large volume of release medium. The initial burst release of the 10 % MTX–PLLA microspheres was more remarkable than that of the 2.5 and 5 % porous MTX–PLLA microspheres, which appeared almost identical. This reveals that a small drug dosage may allow most MTX to be entrapped by the PLLA matrix, while a much higher drug dosage could cause more MTX to be precipitated onto the polymer matrix surface.

After the initial burst release, drug release could be dominated by three factors: (1) the form of combining between the drug and the polymer matrix; most of the left MTX was entrapped into the PLLA matrix; (2) the solubility of the drug in the release medium (MTX is a typical water-insoluble drug); and (3) the degree and speed of infiltration of the microspheres in the release medium, which can be comprehensively affected by the type of material of the polymer matrix, the physical and chemical properties of the release medium, the volume of the porous microspheres, and the diameter of the pores [28, 29]. The first two factors work to slow down the MTX release from the PLLA matrix. The period after 40 h displayed a similar release profile for the porous MTX–PLLA microspheres, demonstrating that different drug dosages do not have a significant effect on the physical properties of porous microspheres (surface morphology, particle volume, and pore size).

All of the above results demonstrate that drug-loaded porous microspheres prepared by a high-voltage electrostatic antisolvent process could offer controlled drug release, which shows great potential for pulmonary drug delivery and therapy for respiratory diseases, such as asthma [30], cystic fibrosis [31], and lung cancer [32].

4 Conclusion

MTX-loaded, large, highly-porous PLLA microspheres were successfully prepared by a high-voltage electrostatic antisolvent process. The obtained MTX-loaded, porous PLLA microspheres exhibited an identifiable spherical shape and a rough surface furnished with open pores, and had a mean particle size of 25.0 μm, MMAD of 3.1 ± 0.2 μm, FPF of 57.1 ± 1.6 %, and porosity of 81.8 %. They offered a sustained MTX release. The XRD and FTIR spectra revealed that no crystallinity or alteration of the chemical structure of the used agents occurred during the high-voltage electrostatic antisolvent process. This study demonstrated that the high-voltage electrostatic antisolvent process has great potential for preparing highly-porous, drug-loaded polymer microspheres to be used in pulmonary drug delivery.

Acknowledgments Financial supports from Natural Science Foundation of Fujian Province (2010J05027 and 2011J01223) and National Natural Science Foundation of China (51103049, 81171471 and 31170939) are gratefully acknowledged.

References

1. Meenach SA, Kim YJ, Kauffman KJ, Kanthamneni N, Bachelder EM, Ainslie KM. Synthesis, optimization, and characterization of camptothecin-loaded acetalated dextran porous microparticles for pulmonary delivery. Mol Pharm. 2012;9:290–8.
2. Arnold MM, Gonnan EM, Schieber LJ, Munson EJ, Berkland C. NanoCipro encapsulation in monodisperse large porous PLGA microparticles. J Control Release. 2007;121:100–9.
3. Ungaro F, Giovino C, Coletta C, Sorrentino R, Miro A, Quaglia F. Engineering gas-foamed large porous particles for efficient local delivery of macromolecules to the lung. Eur J Pharm Sci. 2010;41:60–70.

4. Gupta V, Ahsan F. Influence of PEI as a core modifying agent on PLGA microspheres of PGE1, a pulmonary selective vasodilator. Int J Pharm. 2011;413:51–62.
5. Kwona MJ, Baea JH, Kima JJ, Nab K, Lee ES. Long acting porous microparticle for pulmonary protein delivery. Int J Pharm. 2007;333:5–9.
6. Kirch J, Guenther M, Doshi N, Schaefer UF, Schneider M, Mitragotri S, Lehr CM. Mucociliary clearance of micro- and nanoparticles is independent of size, shape and charge-an ex vivo and in silico approach. J Control Release. 2012;159:128–34.
7. Hadinoto K, Zhu K, Tan RBH. Drug release study of large hollow nanoparticulate aggregates carrier particles for pulmonary delivery. Int J Pharm. 2007;341:195–206.
8. Beck-Broichsitter M, Merkel OM, Kissel T. Controlled pulmonary drug and gene delivery using polymeric nano-carriers. J Control Release. 2012;161:214–24.
9. Oh YJ, Lee J, Seo JY, Rhim T, Kim SH, Yoon HJ, Lee KY. Preparation of budesonide-loaded porous PLGA microparticles and their therapeutic efficacy in a murine asthma model. J Control Release. 2011;150:56–62.
10. Beck-Broichsitter M, Schweiger C, Schmehl T, Gessler T, Seeger W, Kissel T. Characterization of novel spray-dried polymeric particles for controlled pulmonary drug delivery. J Control Release. 2012;158:329–35.
11. Lee J, Oh YJ, Lee SK, Lee KY. Facile control of porous structures of polymer microspheres using an osmotic agent for pulmonary delivery. J Control Release. 2010;146:61–7.
12. Yang Y, Bajaj N, Xu P, Ohn K, Tsifansky MD, Yeo Y. Development of highly porous large PLGA microparticles for pulmonary drug delivery. Biomaterials. 2009;30:1947–53.
13. Kim HK, Chung HJ, Park TG. Biodegradable polymeric microspheres with "open/closed" pores for sustained release of human growth hormone. J Control Release. 2006;112:167–74.
14. Almeria B, Deng W, Fahmy TM, Gomez A. Controlling the morphology of electrospray-generated PLGA microparticles for drug delivery. J Colloid Interface Sci. 2010;343:125–33.
15. Xu Y, Hanna MA. Electrospray encapsulation of water-soluble protein with polylactide—effects of formulations on morphology, encapsulation efficiency and release profile of particles. Int J Pharm. 2006;320:30–6.
16. Zhang W, He X. Encapsulation of living cells in small (approximately 100 μm) alginate microcapsules by electrostatic spraying: a parametric study. J Biomech Eng. 2009;131:074515.
17. Zhou Y, Sun T, Chan M, Zhang J, Han ZY, Wang XW, Toh Y, Chen JP, Yu H. Scalable encapsulation of hepatocytes by electrostatic spraying. J Biotechnol. 2005;117:99–109.
18. Steckel H, Brandes HG. A novel spray-drying technique to produce low density particles for pulmonary delivery. Int J Pharm. 2004;278:187–95.
19. Xie JW, Wang CH. Encapsulation of proteins in biodegradable polymeric microparticles using electrospray in the Taylor Cone-Jet mode. Biotechnol Bioeng. 2007;97:1278–90.
20. Reyderman L, Stavchansky S. Electrostatic spraying and its use in drug delivery-cholesterol microspheres. Int J Pharm. 1995; 124:75–85.
21. Berkland C, Pack DW, Kim K. Controlling surface nano-structure using flow-limited field-injection electrostatic spraying (FFESS) of poly(D, L-lactide-co-glycolide). Biomaterials. 2004;25: 5649–58.
22. Chow AHL, Tong HHY, Chattopadhyay P, Shekunov BY. Particle engineering for pulmonary drug delivery. Pharm Res. 2007; 24:411–37.
23. Giovagnoli S, Blasi P, Schoubben A, Rossi C, Ricci M. Preparation of large porous biodegradable microspheres by using a simple double-emulsion method for capreomycin sulfate pulmonary delivery. Int J Pharm. 2007;333:103–11.
24. Wan F, Møller EH, Yang M, Jørgensen L. Formulation technologies to overcome unfavorable properties of peptides and proteins for pulmonary delivery. Drug Discov Today Technol. 2012;9:e141–6.
25. Huang X, Brazel CS. On the importance and mechanisms of burst release in matrix-controlled drug delivery systems. J Control Release. 2001;73:121–36.
26. Duncan G, Jess TJ, Mohamed F, Price NC, Kelly SM, van der Walle CF. The influence of protein solubilisation, conformation and size on the burst release from poly(lactide-co-glycolide) microspheres. J Control Release. 2005;110:34–48.
27. Wolinsky JB, Colson YL, Grinstaff MW. Local drug delivery strategies for cancer treatment: gels, nanoparticles, polymeric films, rods, and wafers. J Control Release. 2012;159:14–26.
28. Siepmann F, Siepmann J, Walther M, MacRae RJ, Bodmeier R. Polymer blends for controlled elease coatings. J Control Release. 2008;125:1–15.
29. Borgquist P, Korner A, Piculell L, Larsson A, Axelsson A. A model for the drug release from a polymer matrix tablet—effects of swelling and dissolution. J Control Release. 2006;113:216–25.
30. Shrewsbury SB, Bosco AP, Uster PS. Pharmacokinetics of a novel submicron budesonide dispersion for nebulized delivery in asthma. Int J Pharm. 2009;365:12–7.
31. Ibrahim BM, Park S, Han B, Yeo Y. A strategy to deliver genes to cystic fibrosis lungs: a battle with environment. J Control Release. 2011;155:289–95.
32. Anabousi S, Bakowsky U, Schneider M, Huwer H, Lehr CM, Ehrhardt C. In vitro assessment of transferrin-conjugated liposomes as drug delivery systems for inhalation therapy of lung cancer. Eur J Pharm Sci. 2006;29:367–74.